Modeling Turbulent Combustion and Pollutant Formation in Stratified Charge Si Engines

J. M. Duclos, T. Baritaud, A. Fusco

MODELING TURBULENT COMBUSTION AND POLLUTANT FORMATION IN STRATIFIED CHARGE SI ENGINES*

T. BARITAUD and J.-M. DUCLOS

Institut français du pétrole[1]

A. FUSCO

Piaggio SpA[2]

MODÉLISATION DE LA COMBUSTION TURBULENTE ET DE LA FORMATION DES POLLUANTS DANS LES MOTEURS À ALLUMAGE COMMANDÉ AVEC CHARGE STRATIFIÉE.

Une méthode mettant en œuvre des moyennes conditionnelles est appliquée aux modélisations de la combustion et de la formation des polluants dans les moteurs à allumage commandé avec charge stratifiée. Un système d'équations décrit, pendant la combustion, la composition et la température locales du gaz encore non brûlé. Le modèle de flamme cohérente (CFM) a été choisi pour simuler la combustion ; il a été étendu aux combustions en mélange riche ou dilué. Les taux de réactions concernant le NO et le CO sont calculés en prenant comme conditions de référence les températures des gaz brûlés et en considérant deux contributions : un premier terme source est fonction de la densité de flammelettes, de la température et de la composition des gaz frais, et un autre terme source prend en compte les mécanismes d'équilibre et de cinétique dans les gaz brûlés. Les modèles couplés de combustion et de formation des polluants ont été introduits dans le code numérique Kiva-2 et testés avec une géométrie simple de moteur, ceci pour un ensemble de conditions de fonctionnement incluant des variations de richesse, de dilution par des gaz résiduels et de stratification du carburant. Pour les taux de combustion, la capacité du modèle à reproduire les tendances observées est démontrée. L'influence sur le taux de combustion de la flamme laminaire locale est mise en évidence.

L'introduction des moyennes conditionnelles, comparée aux procédures habituelles utilisant des moyennes d'ensembles, conduit à des taux de production de NO et de CO plus importants pendant la combustion, avec pour conséquence des niveaux calculés de NO plus élevés pour la plupart des conditions opératoires, et finalement des niveaux CO similaires à l'issue de la combustion. Les niveaux d'émissions prédits sont comparables aux valeurs mesurées sur moteur.

MODELING TURBULENT COMBUSTION AND POLLUTANT FORMATION IN STRATIFIED CHARGE SI ENGINES

A conditional averaging approach is applied to model combustion and pollutant formation in stratified charge spark-ignition engines. A set of diagnostic equations follows the local composition and temperature of the unburned gases during combustion. The Coherent Flame Model is chosen to simulate combustion. It is

(1) 1 et 4, avenue de Bois-Préau, 92852 Rueil-Malmaison Cedex - France

(2) Pontedera, Italy

* This article was presented at the 26th International Symposium on Combustion, Naples, July 28-August 2, 1996.

extended to rich or diluted combustion. NO and CO reaction rates are computed conditionally based on the burned gas temperature with two contributions: a source term function of the flamelet density and unburned gas composition and temperature, and another source term including equilibrium and kinetic mechanisms in the burned gas. The coupled combustion and pollutant models are implemented in the Kiva-2 code and tested on a simple engine geometry for a set of operating conditions including variation of equivalence ratio, dilution by residual gases and fuel stratification. The ability of the model to reproduce observed trends for combustion rate is demonstrated. The influence of the local laminar flame on the burn rate is pointed out.

A much larger production rate of NO and CO during combustion resulting in higher computed NO levels for most of the operating conditions, and similar final CO levels after combustion completion is observed for the conditional averaging as compared to the usual ensemble averaging procedures. The predicted levels of emissions are comparable to measured engine values.

MODELIZACIÓN DE LA COMBUSTIÓN TURBULENTA Y DE LA FORMACIÓN DE CONTAMINANTES EN LOS MOTORES DE ENCENDIDO CONTROLADO CON CARGA ESTRATIFICADA

Se ha aplicado un método por el cual se implementan los promedios condicionales a las modelizaciones de la combustión y de la formación de contaminantes en los motores de encendido controlado con carga estratificada. Un sistema de ecuaciones describe, durante la combustión, las composiciones y temperaturas locales no consumidos aún. Se ha adoptado el modelo de llama coherente (CFM) para simular la combustión, que se ha aplicado a continuación a las combustiones en mezclas ricas o diluidas. Las tasas de reacciones relativas al NO y al COA se calculan tomando como condiciones de referencia las temperaturas de los gases consumidos y considerando dos contribuciones : un primer término fuente dependiente de la densidad de llamas de reducidas dimensiones, de la temperatura y de la composición de los gases nuevos, mientras que otro término tiene en cuenta los mecanismos de equilibrio y de la cinética de los gases consumidos. Los modelos acoplados de combustión y de formación de contaminantes se han introducido en el código digital Kiva-2 y sometidos a prueba con una geometría sencilla de motos, y ello para un conjunto de condiciones de funcionamiento que incluyen variaciones de riqueza, de dilución por los gases residuales y de estratificación del carburante. Para las tasas de combustión, se ha demostrado la capacidad del modelo para poder reproducir las tendencias observadas. Se hace resaltar de forma evidente la influencia respecto a la tasa de combustión de la llama laminar local.

La introducción de los promedios condicionales, comparada con los procedimientos habituales que utilizan promedios de conjuntos, conduce a tasas de producción de NO y de CO más importantes durante la combustión, y por consiguiente, niveles calculados de NO más elevados para la mayor parte de las condiciones operatorias y, finalmente, niveles de CO similares en la etapa final de la combustión. Los niveles de emisiones previamente considerados son comparables a los valores medidos en el motor.

INTRODUCTION

The design of new efficient and environmentally friendly engines is becoming extremely complex due to the number of solutions that must be tested to find the best trade-off. Three-dimensional modeling of the internal flow can provide a significant reduction of the industrial development phases. However, Computational Fluid Dynamics is not yet used to predict combustion and emissions reliably. The complex nature of engine reacting flows involving multiphase, turbulence, heat and species transfer, combustion and chemical kinetics make it extremely difficult to model.

In spark-ignited engines, combustion occurs in three phases that are ignition, propagation and flame-wall interaction. This takes place in a transient flow formed by the intake process and subsequent mixing. The mixture is made of new admitted air, gaseous fuel originally gaseous or liquid, and burned gases from the previous cycle and/or exhaust gas recirculation. Heat transfer to the wall occurs continuously. At ignition time, the mixture is not homogeneous in concentration and temperature. Experiments (Baritaud and Green, 1986; zur Loye *et al.*, 1987; Wirth and Peters, 1992) have shown that combustion occurs in engines in the flamelet regime. This has stimulated the development of flamelet models to simulate the combustion process.

Pollutants are essentially HC, NO_x, and CO. NO and CO are controlled by the local equivalence ratio and temperature, and formed at the flame front and in the burned gases. HC essentially comes from trapping of the charge in the crevices and in the wall oil film.

NO production is mainly thermal in SI engines. The equivalence ratio is never much larger than one making prompt NO unlikely, as confirmed by the measurements of Bräumer *et al.* (1995). Moreover, the volume occupied by the flamelets where prompt NO could be produced is negligible as compared to the volume occupied by the burned gases. The production of NO_2 is negligible since it is decomposed almost instantaneously due to the high temperature of burned gas. CO production in the flame front is a function of the local equivalence ratio. In most practical CFD calculations, CO kinetics is computed from simple $CO\text{-}CO_2$ equilibrium laws.

In CFD codes such as the Kiva code (Amsden *et al.*, 1989), reaction rates are usually computed based on ensemble averaged values of concentrations and

temperature. Due to their high nonlinearity, the actual reaction rates of pollutants formed essentially in the burned gases may differ a lot from those computed with averaged cell values. This difference is expected to be greatest in the flamelet regime of combustion which is characterized by a thin reacting zone (flamelet) separating the burned and unburned phases of the mixture. Pollutant calculations based on conditional averaging such as used by Gosman *et al.* (1990) for knock calculations should bring significantly improved modeling predictivity. The first goal of this study is to develop new models to extend the range of application of the CFM to stratified charge such as found in actual engines by using a conditional averaging technique. The second goal is to use this conditional approach to compute NO and CO formation. The models developed are implemented in the Kiva-2 code, tested for a range of operating conditions, and compared to engine measurements.

1 EXTENSION OF THE CFM TO STRATIFIED CHARGES

1.1 Application of the Coherent Flame Model to SI engines

The Coherent Flame Model for combustion was developed on empirical basis. The reaction rate is computed as the product of a flame surface density by a laminar flame velocity. A recent development (CFM2a) was to correct the stretch term α with the Interminent Turbulent Net Flame Stretch (ITNFS) model according to Meneveau and Poinsot (1991). It has been successfully applied in SI engines by Boudier *et al.* (1992), Zhao *et al.* (1994), and Torres and Henriot (1994).

Extensions of the CFM to actual situations found in SI engines are required. The laminar ignition LI-CFM initiation model of Boudier *et al.* (1992) and the Flame Interacting with Surface and Turbulence (FIST) wall-flame model of Poinsot *et al.* (1994) have been proposed. The important issue of partial premixing is still to be addressed. The incomplete mixing ahead of the flame front implies that composition and temperature are changing locally and temporally during flame propagation. This causes changes of the local laminar flamelet velocity and burned gas temperature and composition that must be accounted for. Most engine CFD codes solve Favre-averaged equations for species and temperature. The mass and momentum exchanges are computed with a turbulence model (most often the k-ε model) providing turbulent diffusion coefficients, and with laws of the wall for momentum and heat transfer. Obtained quantities are essentially mean scalars and velocity, turbulent kinetic energy and its dissipation.

When combustion begins, new terms are computed: source terms, and flamelet area density with the CFM for instance. For flamelet models involving the assumption of burned and unburned phases in the combusting cells, the original set of solved mean variables is not sufficient to describe the separate properties of the two phases without adding variables. In this work, only the two-phase scalar variables will be computed separately, turbulence and velocity terms being determined unconditionally. The unburned gas properties are solved directly by implementing equations that are not coupled directly with the unconditioned mean values, as proposed by Veynante *et al.* (1991). The added set of diagnostic equations follows the unburned gas properties only to modify the local laminar flame speed S_L and thickness δ_L, and to evaluate some of the CFM terms and compute pollutant kinetic.

1.2 Formulation of the CFM2a for lean combustion

The original Favre averaged set of equations solved for fuel, oxygen, temperature and combustion used in Boudier *et al.* (1992) for lean combustion was:

$$\frac{\partial \bar{\rho} Y_F}{\partial t} + \frac{\partial \bar{\rho} u_k Y_F}{\partial x_k} = \frac{\partial}{\partial x_k}\left(\frac{\mu_t}{\sigma_F}\frac{\partial Y_F}{\partial x_k}\right) - \overline{\dot{\omega}_F} \quad (1)$$

$$\frac{\partial \bar{\rho} Y_O}{\partial t} + \frac{\partial \bar{\rho} u_k Y_O}{\partial x_k} = \frac{\partial}{\partial x_k}\left(\frac{\mu_t}{\sigma_F}\frac{\partial Y_O}{\partial x_k}\right) - s\ \overline{\dot{\omega}_F} \quad (2)$$

$$\frac{\partial \bar{\rho} e}{\partial t} + \frac{\partial \bar{\rho} u_k e}{\partial x_k} = -P\frac{\partial u_k}{\partial x_k} + \frac{\partial}{\partial x_k}\left(\kappa\frac{\partial T}{\partial x_k}\right) + \frac{\partial}{\partial x_k}\left[\frac{\mu_t}{\sigma}\sum_{i=1}^{N} h_i \frac{\partial Y_i}{\partial x_k}\right] - \bar{\rho}\varepsilon + \dot{Q}_c + \dot{Q}_w \quad (3)$$

$$\overline{\dot{\omega}_F} = \rho_u Y_F^0 S_L \Sigma \quad (4)$$

$$\frac{\partial \Sigma}{\partial t} + \frac{\partial u_k K}{\partial x_k} = \frac{\partial}{\partial x_k}\left(\frac{\nu_t}{\sigma \Sigma}\frac{\partial \Sigma}{\partial x_k}\right) + S - D \qquad (5)$$

with $D = \beta\ \rho_u Y_F^0 S_L / \overline{\rho} Y \Sigma^2$

and $S = \alpha\ \varepsilon / k\ f\left(\frac{u'}{S_L},\ \frac{L}{\delta_L}\right)\ \Sigma$

with the ITNFS stretch.

The expression for D was slightly different than expressed here, but giving the same results with the usual turbulence and flame conditions in SI engines. This set was completed by the usual equations for mass, momentum, and a k-ε model for turbulence.

The previous set of equations was computed using mean properties in the cells, except for the evaluation of S_L which was estimated from the unburned gas properties taken for a uniform equivalence ratio mixture, and with an unburned gas temperature obtained assuming isentropic compression after ignition timing and neglecting heat transfer to the walls during combustion.

Moreover, it was assumed that no residuals were trapped in the charge.

1.3 Extension to rich and diluted mixture and diagnostic equations for the unburned phase

Favre-averaged diagnostics equations that are not directly coupled to equations (1) to (5) are added to follow the evolution of the unburned gases ahead of the flamelets. $Y_{F,u}$ and $Y_{O,u}$ and are respectively the mass of fuel and oxygen in the unburned gases divided by the total mass.

Y_F^u and Y_O^u are respectively the mass of fuel and oxygen in the unburned gas divided by the mass of unburned gas. h_u and T_u are the enthalpy and temperature in the unburned gases:

$$\frac{\partial \overline{\rho} Y_{F,u}}{\partial t} + \frac{\partial \overline{\rho} u_k Y_{F,u}}{\partial x_k} = \frac{\partial}{\partial x_k}\left(\frac{\mu_t}{\sigma_F}\frac{\partial Y_{F,u}}{\partial x_k}\right) - \overline{\dot{\omega}_{F,u}} \qquad (6)$$

$$\frac{\partial \overline{\rho} Y_{O,u}}{\partial t} + \frac{\partial \overline{\rho} u_k Y_{O,u}}{\partial x_k} = \frac{\partial}{\partial x_k}\left(\frac{\mu_t}{\sigma_F}\frac{\partial Y_{O,u}}{\partial x_k}\right) - \frac{s}{\Phi}\ \overline{\dot{\omega}_{F,u}} \qquad (7)$$

$$\overline{\dot{\omega}_{F,u}} = \rho_u Y_F^u S_L \Sigma \qquad (8)$$

$$\frac{\partial \overline{\rho} h_u}{\partial t} + \frac{\partial \overline{\rho} u_k h_u}{\partial x_k} = \frac{\partial}{\partial x_k}\left(\frac{\mu_t}{P_r}\frac{\partial h_u}{\partial x_k}\right) - \overline{\rho}\varepsilon + \frac{\overline{\rho}}{\rho_u}\frac{\partial p}{\partial t} + \dot{Q}_{w,u} \qquad (9)$$

and the flame surface density destruction term of equation (5) becomes $D = \beta\ \rho_u Y_O^u S_L / \overline{\rho} Y_O \Sigma^2$ when the equivalence ration is greater than 1. S_L and δ_L are then deduced from the computed unburned equivalence ratio and temperature.

This formulation of D can lead to some trouble since it is shaped to become large when the limiting reactant disappears, which is expected for oxygen in the rich case. However, engine calculations always include post-flame gas kinetics such as CO-CO_2 for instance, which produce O_2 which should not be considered in D. Then, a better formulation is $D = \beta\ \rho_u Y_O^u S_L / \overline{\rho} Y_{O,u} \Sigma^2$, which is not influenced by the burned gas composition.

Y_F^u and Y_O^u and can be evaluated from $Y_{F,u}$ and $Y_{O,u}$ if the ratio of nitrogen to oxygen is constant in the unburned gases.

In the set of equations (6) to (9), the assumption is that exchanges in the gas occur independently in the burned and unburned gases, except through the reaction rate at the interface, which is fully consistent with the flamelet regime. Recent Direct Numerical Simulation of flame-wall interaction by Bruneaux *et al.* (1995) whith locally low reaction rates have shown that the flamelet concept was still valid, and that there was no inert mixing across the flamelets. Another assumption underlying these equations is that exchange fluxes are statistically occurring through the whole external area of the cell.

Equation (9) describing the evolution of the enthalpy is retained instead of an energy equation since it provides an easier way to integrate the contribution of combustion heat release through the total pressure variation as formulated in the third term on the RHS. It also supposes a Lewis number of 1 which is the case in Kiva-2. The last term $Q_{w,u}$ representing heat transfer of the unburned gases with the walls is taken as the heat transfer computed with the model of Diwakar (1984) such as implemented by Gilaber and Pinchon (1988), but taking into account the unburned gas temperature. The unburned gas temperature is deduced directly from the enthalpy.

The laminar flame speed S_L is a function of the equivalence ratio and temperature in the unburned gases, as well as its thickness δ_L. It also depends on the burned gas temperature which can be estimated from the state of the computed cell. Finally, there is also a dependence on the pressure, and on the amount of residual gases in the unburned gases. δ_L is computed according to Blint's work (1986), and S_L from the correlation of Metghalchi and Keck (1982) which accounts for residuals.

2 NO AND CO FORMATION

NO and CO are formed and evolve both in the flame front and in the burned gases. Typical of SI engines is the fact that the volume of the laminar flamelets is small as compared to the volume of the hot burned gases which are hot for a long time. Hence, it is expected that most of the pollutant kinetics is controlled by the phenomena in the bulk of the burned gases. However, the possibility of creation of pollutants directly in the flamelet and acting as a local and temporal source term must be considered.

Complex chemical schemes are very dependent on temperature, composition and pressure while the accuracy of these computed quantities in CFD codes is presently limited. Hence, schemes with a limited number of steps and species allowing a reasonable predictivity versus computing time trade-off are preferred.

Although flamelets are thin, CFD codes predict average statistical variable values in each cell of the domain. This produces a large combustion zone with a weak temperature gradient including intermediate temperatures that do not exist in individual engine cycles while the quantity of interest for computing pollutants is that of the burned gases.

2.1 Determination of the burned gas temperature

The procedure previously described to extend the CFM to stratified charge involves the computation of the unburned gas temperature T_u and composition $Y_{j,u}$, along with the averaged values in the domain. The burned fraction of each cell can be obtained from the ratio $b = Y / Y_F^u$. Hence, it is possible to compute the enthalpy in the burned gases by:

$$h_b = \frac{h - bh_u}{1 - b} \tag{10}$$

from which can be computed.

For very small burned fraction, equation (11) can be ill-determined. Then if $c < 0.01$, the burned temperature of the cell is evaluated as if it has completely burned adiabatically with the correction for chemical equilibrium described in the next section. The influence of this approximation on pollutant calculations is marginal.

2.2 Pollutant kinetics

A new approach is developed to compute NO and CO for both rich or lean combustion. First, a source term of species created at the flamelets is determined. From the composition of the unburned gases and the thermodynamic state of the cell, it is assumed that the flamelets produce species from which atoms production corresponds to the burn rate in the cell as computed by $\overline{\dot{\omega}_{C_j,u}} = \rho_u Y_{C_j}^u S_L \Sigma$ from the CFM model.

These species are distributed in product molecules and radicals corresponding to the equilibrium mechanism (11) proposed by Meintjes and Morgan (1987) at the burned gas temperature:

$$\begin{aligned} &2N \leftrightarrow N_2 \\ &2H \leftrightarrow H_2 \\ &2O \leftrightarrow O_2 \\ &H_2 + O_2 \leftrightarrow 2OH \\ &2OH + O_2 \leftrightarrow H_2O \\ &CO + O_2 \leftrightarrow CO_2 \end{aligned} \tag{11}$$

The assumption of equilibrium may appear too simple. However, SI engine flamelets are very thin, and if the equilibrium is reached at a distance of a few flame widths, it can still be considered as a flamelet source term.

In the burned gases, the same equilibrium mechanism is used, but without the CO-CO_2 contribution. It is coupled to a kinetic mechanism for slower reactions using a numerical implicit procedure proposed by Ramshaw and Chang (1995). The kinetic reactions are for thermal NO (extended Zeldovitch) and CO and CO_2. The purpose of kinetic CO-CO_2 is to deal with lower temperature, close to walls for instance. The

constants are from Seshadri and Williams (1994) and Heywood (1988):

$$\begin{aligned} CO + OH &\leftrightarrow CO_2 + H \\ N + O_2 &\leftrightarrow NO + N_2 \\ N_2 + O &\leftrightarrow NO + N_2 \\ N + OH &\leftrightarrow NO + H \end{aligned} \quad (12)$$

The chemistry is supposed frozen below 1300 K.

Chemistry is conditionally computed on the burned gas fraction in each cell based on the amount of each specie, the estimated burned gas temperature, and the pressure.

3 ENGINE SIMULATIONS

The conditionally averaged combustion and pollutant models have been implemented using KMB which is an extended version of Kiva-2 (Habchi and Torres, 1993), and applied in a 2D mesh representative of the cylindrical engine geometry of Baritaud (1989). This engine has a bore x stroke of 86 x 82 mm and a compression ratio of 6.2. The clearance height at TDC is 15.4 mm. A swirl flow of intensity 3.8 and close to solid body rotation was observed at Bottom Dead Center. The volumetric efficiency for all simulated cases is 0.5. The spark-plug is located on the cylinder axis 7.5 mm below the head and the spark energy was 20 mJ (2 ms x 10 w). The fuel is propane. The axi-symetric domain computed is a plane delimited by the cylinder axis and the cylinder liner, and the piston and head surfaces. The turbulence level at ignition timing and 1200 rpm was determined to be around 2 m/s. The ignition source is located on the chamber axis, 7.5 mm below the flat head.

The computational mesh is refined near the wall and the ignition point located on the chamber axis was 40 cells in the radial direction and 42 in the axial direction. The work of Boudier *et al.* (1992) had shown that this was sufficient to have a grid-independent combustion simulation. The LI-CFM model of the same authors was used. The FIST flame-wall model is implemented to provide a correct behavior of the combustion rate close to the walls.

The runs are conducted starting at compression BDC. k, ε and a transverse swirl velocity profile representative of the measured values are imposed. The concentration fields are also imposed at BDC, according to realistic values measured by Deschamps *et al.* (1994), and in the validity range of the S_L correlation.

3.1 Stratified charge combustion

Numerical tests were conducted to assess the validity of the equation sets and coding. The equation system (6) to (8) with the new formulation of the destruction term D was compared in the case of homogeneous rich and lean combustion to the original (1) to (5) set. Not activating the conditional unburned enthalpy equation (keeping the approximation of an unburned temperature corresponding to an isentropic compression starting at ignition), they gave similar results. The final amount of the excess specie (fuel Y_F or Y_O oxygen) gave also the right value. The conditional enthalpy equation was tested by comparing the evolution of the predicted unburned temperature with the adiabatic compression temperature during combustion. This was done for an adiabatic homogeneous mixture combustion with $Q_{w,u} = 0$. The two unburned temperature stayed within 1 K. Finally, the simple correction of S_L with residuals gases showed no application problems.

Calculations of stratified charge combustion are now presented. They involve variation of the stratification of fuel, residuals, and heat transfer effects described in Table 1. At this stage, pollutant chemistry in the burned gases is not considered to provide a clearer understanding. The wall temperature is 400 K.

TABLE 1

Computed operating conditions for stratified charges

HFHT	Homogeneous mixture, $\Phi = 0.9$
VFHT	Vertical fuel stratification, $\Phi = 1.0$ at spark/cylinder axis and 0.8 at liner side wall at -25 CAD
HOFHT	Horizontal fuel stratification, $\Phi = 1.1$ at top wall and 0.7 at lower wall at -25 CAD
HFIT HFCT	Homogeneous mixture, $\Phi = 0.9$, isentropic unconditioned and conditioned T
VFIT VFCT	Vertical fuel stratification, $\Phi = 1.0$ at spark/cylinder axis and 0.8 at liner wall at -25 CAD, isentropic unconditioned and conditioned T

The effect of a stratification of the fuel charge is shown on Figure 1 by comparing burned mass fractions for cases HFHT (homogenous), VFHT (vertical fuel stratification) and HOFHT (horizontal fuel stratification). Stratification patterns imposed at TDC result in the stratification amplitude at TDC given in Table 1. The ability of the model to reproduce the expected trends in stratified charges appears clearly.

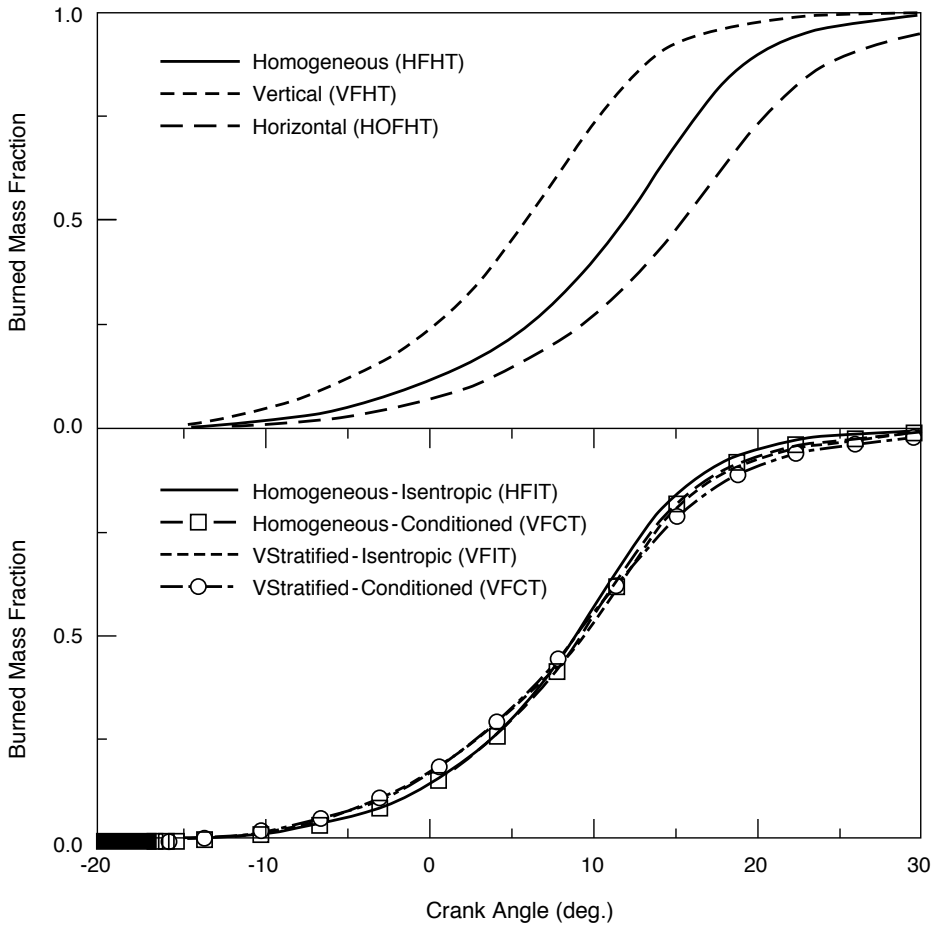

Figure 1

Fuel burned mass fraction in the combustion chamber:
Effect of fuel stratification: homogenous HFHT, vertically stratified VFHT, and horizontally stratified HOFHT
Effect of isentropic unconditioned/conditioned temperature: homogenous HFIT, HFCT and vertically stratified VFIT, VFCT.

As found experimentally by Deschamps *et al.* (1994), igniting in a stratified mixture on the richer side favors the global combustion speed as compared to the homogeneous case. An horizontal stratification gives a lower heat release rate. The fields of S, S_L, and $\overline{\dot{\omega}_F}$ when the flame is in the middle of the chamber for the horizontal stratification case HOFHT are plotted on Figure 2. At the top of the chamber with a higher equivalence ratio, S_L is larger than at the bottom. In the leaner and lower part of the chamber, the flame surface density Σ is larger. The resulting combustion rate is larger in the region of larger S_L, showing the importance of the laminar flame speed even in the very turbulent environment of engine chambers. This emphasizes the fact that it is crucial to have an accurate determination of S_L to predict well the combustion rate, and that the conditional averaging procedure proposed in this work is necessary. The effect of using a conditional temperature to determine S_L is now discussed. This time, Y_F^u and Y_O^u are directly solved as tracers without source terms. A new 3D version of the LI-CFM ignition model equivalent to the 2D LI-CFM for the present calculation is activated.

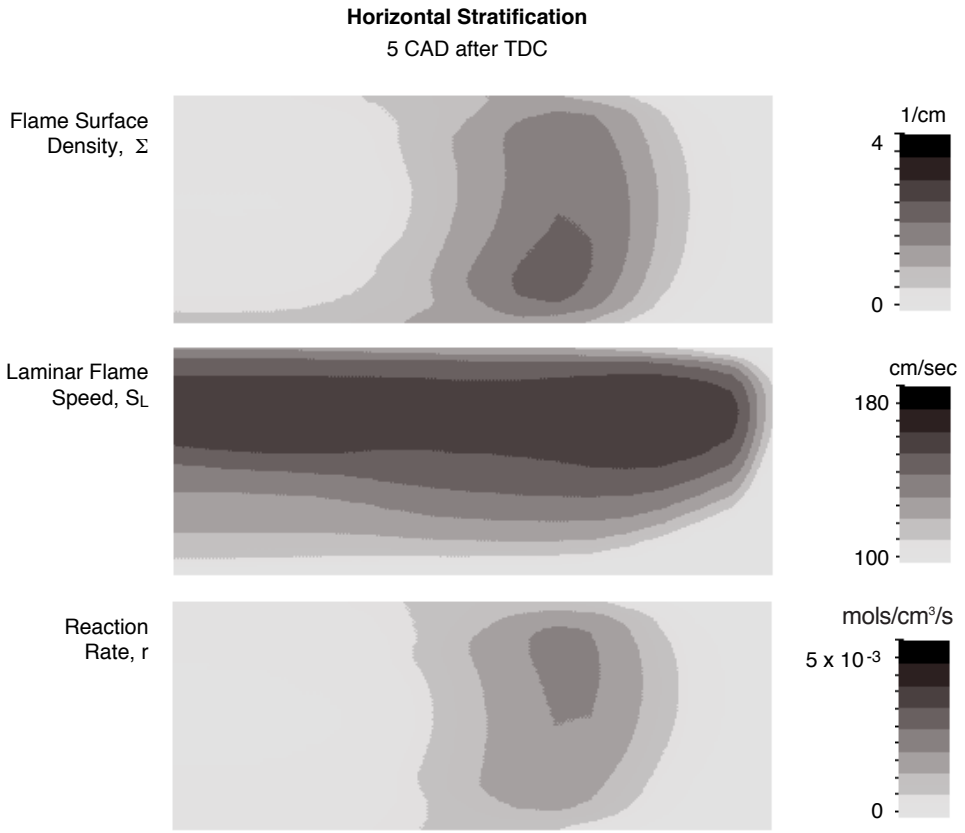

Figure 2

Spatial distribution of flame density Σ, laminar flame speed S_L, and reaction rate $\overline{\dot{\omega}_F}$ for case HOFHT with horizontal fuel stratification. 5 CA after TDC. Average equivalence ratio $\Phi = 0.9$.

The effect of conditioning the unburned temperature instead of using an isentropic evolution to compute the laminar flame speed has an effect mostly in the second half of the combustion process (Fig. 1).

The reason is that heat exchange with the walls is the unique source of temperature inhomogeneity in the test cases, and affects more the gases close to the walls. In actual engines, there would be more temperature variations across the chamber due to mixing with residuals and more complicated chamber shapes. The time evolutions observed in a cell 1 mm away from a wall on Figure 3 shows that 20 to 30 K differences between isentropic and conditioned temperature are obtained and lead locally to 10 to 20% differences in laminar flame speed.

3.2 Pollutant formation

To compute the pollutants conditionally, the same numerical configuration is retained. The chemical equilibrium and kinetics schemes already presented are coupled to this system to observe the evolution of NO and CO.

Runs are made for homogeneous charges with Φ ranging from 0.85 to 1.1, and rpm 1200 and 2400, and vertically and horizontally stratified charges with mean Φ of 0.85 and 1.0. Comparisons between unconditioned and conditioned pollutant calculations are made. For the non-temperature conditioned cases, the coupled kinetic systems are used based on the averaged cell temperature while the source terms at the flamelets were only CO_2 and H_2O.

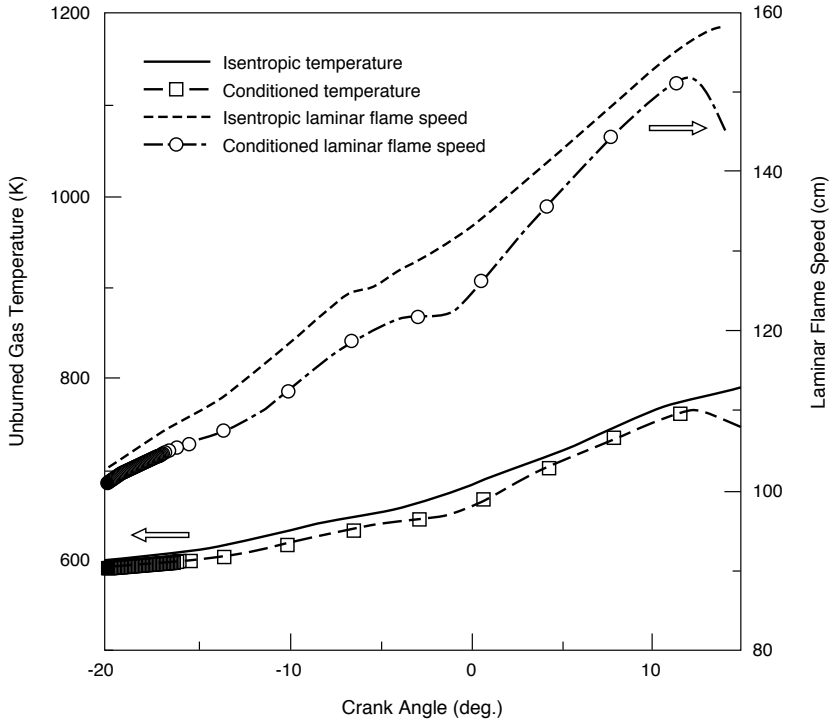

Figure 3

Evolution of isentropic and conditioned unburned temperature Tu and resulting S_L in a cell 1 mm away from a 400K wall for the fuel stratified case VFCT.

Detailed engine measurements not being available, the pollutant predictions of the simple 2-D engine case will be compared to 4-valve commercial engine typical exhaust engine levels measured at *IFP* and reported in Table 2. In this engine, it is possible to stratify the charge as shown by Deschamps *et al.* (1994). The numbers are indicative of trends when varying parameters, but care should be taken when doing comparison with the present calculations (different geometry, turbulence, stratification, spark location and timing, etc.).

During combustion, the new conditioned kinetic scheme and procedure predict a larger rate of production of CO (Fig. 4).

TABLE 2

Measured exhaust emissions in 4-valve SI engine. 1200 rpm, 441 cm^3, compression ratio 8.7, volumetric efficiency 0.6, optimized ignition timing for each point, fuel iso-octane. On the 3 right columns, corresponding configurations of Table 2 and computed values from Figures 4 and 5 with the modeled flat head engine

Measured and computed cases and values 4-valve engine configurations	**NO ppm**	**CO (%)**	**Ign. timing**	**"Equivalent" computed case**	**NO ppm**	**CO (%)**
Homogeneous charge, medium turbulence, side ignition, Φ = 1	3 128	0.43	- 11	HFCT, Φ = 0.99	3 660	0.23
Homogeneous charge, high turbulence, side ignition, Φ = 1	3 458	0.24	- 6.5	HFCT, Φ = 0.99	3 660	0.23
Stratified charge, medium turbulence, side ignition on rich side, Φ = 0.9	3 000	0.64	- 16	VFCT, Φ = 0.85	4 400	0.05
Stratified charge, medium turbulence, side ignition on rich side, Φ = 0.8	5 700	0.2	- 17	VFCT, Φ = 0.85	4 400	0.05
Stratified charge, medium turbulence, side ignition on rich side, Φ = 0.8, 15% EGR	293	0.21	- 25	VFCT, Φ = 0.85, 20% residuals	160	0.03

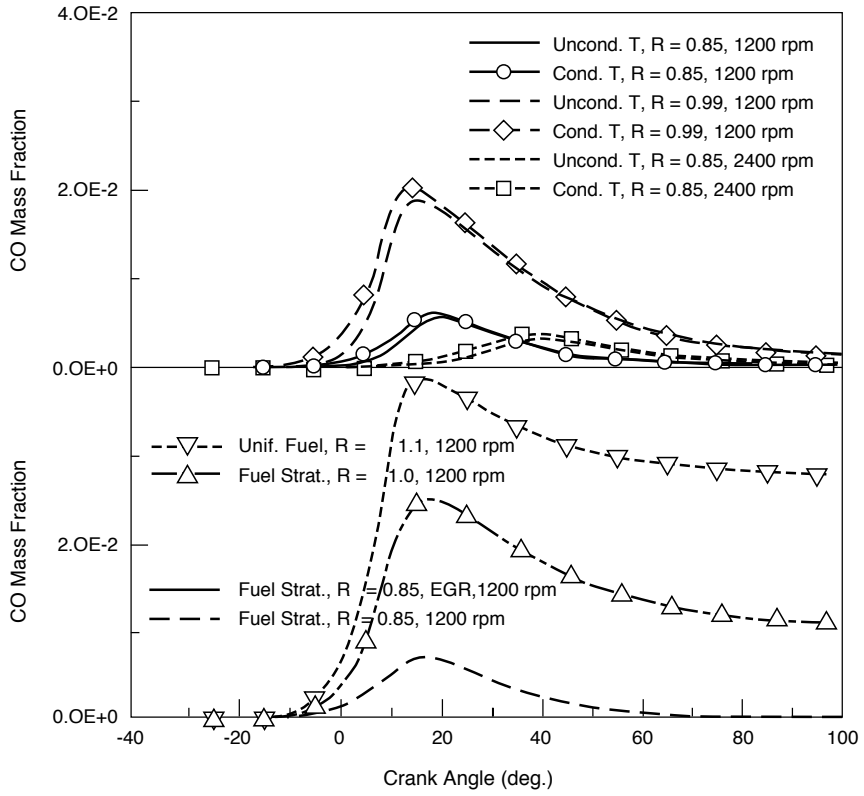

Figure 4

CO integrated relative mass in the combustion chamber.

However due to the long residence time of the chemical species in the fully burned gases, the values given by the old and new procedure become almost equal after a certain delay following combustion completion. The end values are close to the equilibrium values for all the lean cases. The equivalence ratio changes predict evolution and levels close to the measured values of Table 2, the absolute levels being lower in the modeled chamber, with $0.85 < \Phi < 1.1$ since the contribution of the unburned HC chemistry present in the experiment is not considered. For the same reason, the calculations do not predict CO for lean combustion. The model shows its ability to reproduce the CO elevation for a rich case and a horizontally stratified charge case with an equivalence ratio ranging between 1.1 and 0.9 at ignition time. The production rate for a lean vertically stratified case with average Φ of 0.85 with ignition on the rich side produces also more CO than the homogeneous case. Finally, adding 20% residual gases while keeping the same volumetric efficiency produces an expected decrease of CO due to diluted and leaner combustion. The difference between the conditioned and unconditioned runs for the evolution of NO shown on Figure 5 depends on the operating conditions. With an homogeneous equivalence ratio 0.99, NO is not much influenced by the conditioning. However, for the leaner homogenous cases at $\Phi = 0.85$ were NO is expected to peak, NO formation rate is much higher. This is due to the fact that with the conditioning procedure the production of NO begins in a cell as soon as some hot burned gas exists. The resulting levels late after combustion completion can differ by as much as 20% with the tested conditions. The predominance of the NO thermal kinetics is reflected in the lower NO level at higher rpm where there is less evolution time available in seconds for a similar number of CADs. The homogeneous rich case behaves well too, with a marked reduction of NO. In all cases, the obtained levels are very close to the measured ones, and more important the influence of the varied parameters are similar. Lower value in the lower compression ratio flat-head engine could be expected, but it is probable that the weak wall heat transfer considered in the computations is partially compensating. Both computed fuel stratified cases produce less NO, with more difference for the leaner case, although there was no attempt to optimize ignition timing. Adding 20% residuals produces a dramatic

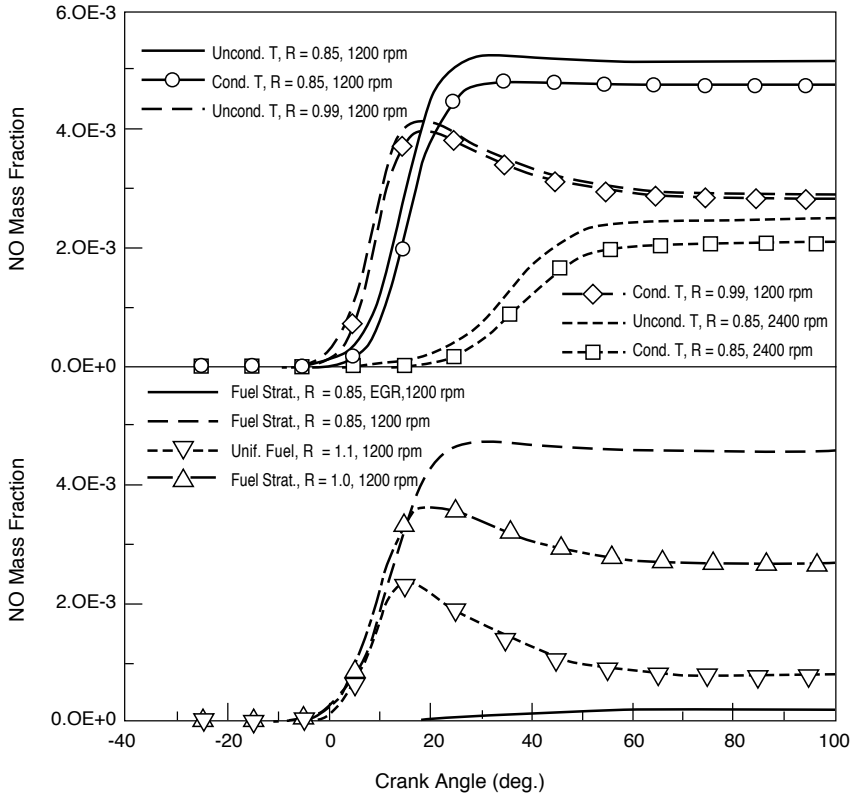

Figure 5

NO integrated relative mass in the combustion chamber.

decrease of NO due to both diluted charge an delayed combustion causing very low burned gas temperature.

CONCLUSION

The conditional approach developed to compute the scalar properties (equivalence ratio, temperature, dilution) of the unburned gases in the flamelet regime coupled to the Coherent Flame Model, has been shown to give the capability to CFD codes to simulate the combustion of stratified charge such as found in SI engines. It is valid in the flamelet combustion regime, and for all equivalence ratio if combustion stays in the premixed mode. The observed behavior is very similar to the experimental observation, although there are no available relevant data set to quantify in detail the accuracy of the prediction. It will be necessary to design specific experiments where flow and stratification are well controlled to validate stratified charge combustion models. Improvements can be sought, such as the use of more accurate laminar flame speed versus gas composition, pressure and temperature or handling of close to extinction combustion.

The calculation of NO and CO with a chemical approach coupling equilibrium and kinetic schemes, source term at the flamelet and bulk reaction conditioned by the actual temperature of the burned gases in the combusting cells permit to obtain more realistic results than conventional simple ensemble averaged procedures. Computations of a set of SI engine typical lay-outs for charge stratification have shown the ability of the new conditioned combustion and pollutant approach to reproduce the pollutant production behavior and level usually measured in engines. There is indeed a lack of local measurement of pollutant inside combustion chamber which exclude a direct validation of the models. Improvements of chemical schemes could be easily included in the presented approach.

Despite the lack of detailed validation by relevant experiments, the present approach is a significant step towards modeling of combustion and pollutants in engines. The major features of engine combustion and NO and CO formation in actual SI engines have been taken into account, and the simulation system obtained certainly already allows for an estimation of the impact of engine design on performances and emissions.

NOMENCLATURE

S_L	Laminar flame speed
δ_L	Laminar flame thickness
Σ	Flame surface density divided by the mass in the cell
$\dot{\omega}_F$	Reaction rate of the fuel
S	Production/stretch term of flame surface
D	Destruction/curvature term of flame surface
s	Stoichiometric ratio
$\dot{Q}_w$	Heat transfer to the wall
$\dot{Q}_c$	Chemical heat release
Φ	Equivalence ratio
$Y_{F,u}$	Mass of unburned fuel divided by the mass in the cell
Y_F^u	Mass of unburned fuel divided by the mass of the unburned gases in the cell
e_u	Energy of the unburned gases divided by the mass in the cell
k	Kinetic energy of the turbulence
ε	Dissipation rate of the kinetic energy
μ_t	Turbulent viscosity
P_r	Turbulent Prantdl number
σ_F	Turbulent Schmidt number for the fuel
u	Subscript or superscript for the unburned gas phase properties
b	Subscript or superscript for the unburned gas phase properties.

No subscript or superscript for averaged quantities in the cells. In the equations, the variables are essentially Favre averages, and the usual tilde symbol is omitted.

REFERENCES

Amsden A.A., P.J. O'Rourke and T.D. Butler (1993), *Report LA-11560-MS*. Los Alamos Ntl. Laboratories.

Baritaud T. and R.M. Green (1986), *SAE Paper* 860025.

Baritaud T. (1989), *SAE Paper* 892098.

Blint R.J. (1986), *Combust. Sci. & Tech.*, **49**, p. 79.

Boudier P., S. Henriot, T. Poinsot and T. Baritaud (1992), *24th Symp. (Int.) on Combustion*. The Combustion Institute, *Pittsburgh,* pp. 503-510.

Bräumer A., V. Sick, J. Wolfrum, V. Drewes, M. Zahn, and R. Maly (1995), *SAE Paper* 952462.

Bruneaux G., T.J. Poinsot and J. Ferziger (1996), to appear in *Comb. and Flame*.

Deschamps B., R. Snyder and T.A. Baritaud (1994), *SAE Paper* 941993.

Diwakar R. (1984), *SAE Paper* 840230.

Gosman A.D., C.J. Marooney and H.G. Weller (1990), *Comodia 1990*. pp. 59-64.

Habchi C. and A. Torres (1992), *First European CFD Conference Symposium*. pp. 502-512.

Heywood J.B. (1988), in *Internal Combustion Engine Fundamentals*. McGraw-Hill.

Meintjes K. and A.P. Morgan (1987), *General Motors Research Publications* GMR-5827.

Meneveau C. T. and Poinsot (1991), *Comb. and Flame*. **86**, pp. 311-332.

Metghachi M. and J.C. Keck (1982), *Comb. and Flame*. **48**, pp. 191-210.

Poinsot T., D. Haworth and G. Bruneaux (1993), *Comb. and Flame*. **95**, pp. 118-133.

Ramshaw J.D. and C.H. Chang (1995), *J. of Comp. Physics*. **116**, pp. 359-364.

Seshadri K., F.A. and Williams (1994), in *Turbulent Reacting Flows* (Libby and Williams Ed.). Academic Press, London.

Torres A., S. and Henriot (1994), *Comodia 1994*. pp. 151-156.

Veynante D., F. Lacas, E. Maistret and S.M. Candel (1991), *7th Turbulent Shear Flows*. Springer-Verlag, Berlin. pp. 367-378.

Wirth M. and N. Peters (1992), *24th Symp. (Int.) on Combustion*. The Combustion Institute, Pittsburgh. pp. 493-501.

Zhao X., R. Matthews and J. Ellzey (1994), *Comodia 1994*.

Final manuscript received in June 1997